High-Speed Impact between a Liquid Drop and a Solid Surface

F. J. HEYMANN

Development Engineering, Steam Division, Westinghouse Electric Corporation, Lester, Pennsylvania 19113

(Received 23 June 1969; in final form 22 August 1969)

The dynamics of high-speed impact between a compressible liquid drop and a solid surface are reviewed. Previous estimates for the maximum impact pressure have been based on one-dimensional approximations. This paper presents a two-dimensional approximation, adapted from a closely related analysis of the oblique impact between two solid plates. This is valid only for the "initial" phase of the impact during which the expanding shock front generated by the impact still remains attached to the target surface, and no lateral outflow takes place. The derivations assume a linear relationship between shock velocity and particle velocity change across the shock front. Numerical results are presented for water and sodium, and can be generalized as follows: The contact pressure remains substantially equal to the one-dimensional pressure until the contact angle ϕ at the edge has reached about half of its critical value, at which the assumed model beaks down and lateral outflow must initiate. As this critical condition is further approached, the contact edge pressure increases progressively, and its critical value P_c is taken as the maximum impact pressure. The ratio $P_c/\rho_0 C_0 V_0$ always exceeds about 2.75 exhibiting a minimum in the vicinity of $V_0/C_0=0.2$, where ρ_0 and C_0 are the density and acoustic velocity of the liquid, and V_0 is the impact velocity. These pressures are considerably higher than have been heretofore supposed, but circumstantial experimental evidence supports the present results.

I. INTRODUCTION

Material damage and erosion, caused by the impact of liquid drops, has long been a problem for the steam turbine designer and operator. The same has recently become of increasing concern in the aerospace industry, both because of serious rain erosion problems sustained by supersonic aircraft and missiles, and because of anticipated blade erosion problems in turbines of space power plants using liquid metals as the working fluid.

Unfortunately, we still lack any rigorous solution for the flow patterns and impact pressures developed in the collision between a liquid drop and a plane solid surface. The usual assumptions result in only a rough approximation of the impact pressure. In order to permit a better understanding of the effect of such collisions on the target material, it would be most desirable to know the exact time-dependent pressure distribution at the impact interface, or at least the exact value of the maximum instantaneous impact pressures generated.

The purpose of this paper is to put together a qualitatively accurate picture of the collision process between a liquid drop and a rigid surface, and to present new quantitative results for the maximum impact pressure generated. The latter are based on an analysis which Walsh *et al.*[1] had developed for a somewhat analogous phenomenon.

II. BACKGROUND

One-Dimensional Liquid–Solid Impact

The most frequently used approximations to the pressure developed in liquid–solid impact are based on one-dimensional "waterhammer" or elastic impact theory. When the solid surface can be assumed rigid, this results in

$$P=\rho_0 C_0 V_0, \tag{1}$$

where ρ_0 and C_0 are the density and acoustic velocity of the undisturbed liquid and V_0 is the impact velocity. This well-known expression can easily be derived from momentum considerations, if one assumes that upon impact a plane pressure or shock wave of magnitude P propagates into the impinging liquid body at a relative velocity C_0, progressively bringing to rest each liquid "layer" as it passes through.

The events which actually occur, when a liquid drop impacts at high speed, differ from this simple model in two important respects:

(1) The velocity of propagation of a shock wave is not an invariant, as is assumed in Eq. (1), and only at very low shock pressures can it even be approximated by the acoustic velocity of the undisturbed liquid. More rigorously, the shock wave velocity C must be treated as a function of the pressure itself.

A one-dimensional analysis incorporating a variable shock wave velocity, for both rigid and elastic solid targets, was recently presented.[2] We shall make use of some of these results later, but must restrict ourselves to impacts on a rigid target. For this case, the impact pressure was shown[2] to be approximated by

$$P=\rho_0 C_0 V_0[1+k(V_0/C_0)], \tag{2}$$

where k is a constant for the liquid considered.

(2) Conditions are *not* one dimensional. Contact is initially made at one point and the contact area grows as the impact process continues. The pressure or shock front generated by the impact is domed, not plane, and

[1] J. M. Walsh, R. G. Shreffler, and F. J. Willig, J. Appl. Phys. 24, 349 (1953).

[2] F. J Heymann, J. Basic Eng. 90, 400 (1968).

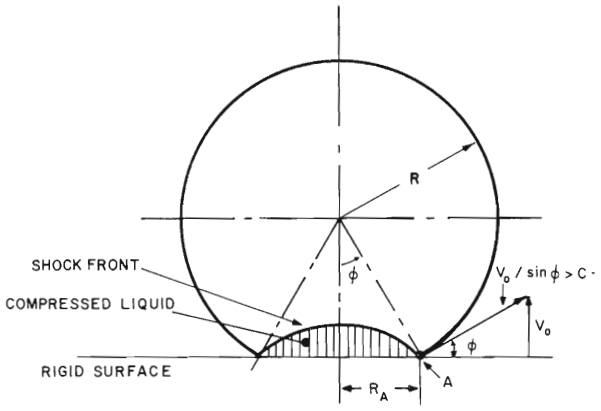

FIG. 1. Initial (compressible) stage of impact, according to Bowden and Field (Ref. 6).

there is a radial component of particle motion. (Eventually, there is gross lateral spreading flow.)

The effects of the roundness of the drop, and of the pressure dependence of C, are significant: We shall see that the simple waterhammer pressure, given by Eq. (1), underestimates the actual peak impact pressures by a factor of at least 3.

Liquid–Solid Impact of Curved Surfaces

Let us now review previous work, and construct the current state of knowledge, relating to the impact of liquid drops. Savic and Boult[3] presented a mathematical analysis of the low-speed impact and spreading of a spherical liquid drop on a rigid surface, but it neglects compressibility of the liquid and consequently predicts infinite pressure at the first instant of impact. The analysis therefore is not valid while compressibility effects are predominant in the liquid response.

An approximate analysis, based on a combination of flow arguments and pressure wave arguments, was presented by Engel.[4] This culminated in the equation

$$P=(\alpha/2)\rho_0 C_0 V_0 \qquad (3)$$

and a later paper[5] gave the value $\alpha=0.41$ for the impact of a round drop on a rigid surface. Strictly speaking, this equation was *not* intended to represent the maximum pressure developed, but it has often been cited as such, thus giving rise to the impression that the impact of a round drop results in much lower contact stresses than predicted by one-dimensional theory, whereas, as will be shown, the opposite is really true. Moreover, the arguments presented in Refs. 4 and 5 assume that lateral outflow from the impact zone begins immediately, an assumption not shared by most subsequent thinking on this matter.

It is now widely accepted that a crucial feature of the impact process, between a curved liquid surface and a plane solid surface, is the existence of an initial stage during which the response of the liquid is entirely compressible, and no gross spreading or lateral outflow occurs. This was first pointed out by Bowden and Field,[6] and justified by a simple argument which can be paraphrased as follows:

Initially, the perimeter of the liquid/solid interface moves tangentially outward at a speed which exceeds the velocity of propagation of the shock waves generated by the impact. The resulting shock front, therefore, remains attached to the solid surface; and the compressed liquid, being bounded entirely by the solid surface on one side and by the shock front separating it from undisturbed liquid on the other, cannot flow out. It is only when shock waves overtake the interface perimeter, and reach a "free" surface, i.e., when the shock front becomes detached, that lateral flow is able to begin.

While this picture can be accepted qualitatively, Bowden and Field's quantitative conclusions, which also have been widely cited, are based on an oversimplified analysis. These conclusions (see Fig. 1) are (1) that the limiting contact angle for the initial stage, at which the shock front becomes detached, is given by

$$\sin\phi = V_0/C, \qquad (4)$$

where C is the velocity of propagation of the shock wave, and (2) that until this limit is reached, the impact pressure will be uniform and equal to that corresponding to a one-dimensional analysis. We shall later see that these conclusions are not quite correct.

A slightly more accurate picture can be inferred from a contribution by Skalak and Feit.[7] This deals with the impact of a blunt solid body onto the surface of a semi-infinite compressible fluid; but if the radius of curvature of the solid body surface is large compared to the dimensions of the contact area, the results should apply at least qualitatively to the droplet problem, so long as the contact radius is still small compared to the drop radius. Skalak and Feit's acoustic wave equation approach is restricted, however, to an invariant propagation velocity C_0, to low values of the Impact Mach Number $M_0=V_0/C_0$, and to small "penetrations" of the liquid surface. The significant conclusions are:

(1) No gross flow or splashing occurs until the pressure waves can overtake the contact area perimeter, and during this initial period the *average* pressure over the contact area equals the one-dimensional pressure $\rho_0 C_0 V_0$.

(2) The pressure distribution is nonuniform during the initial period, with pressures maximum at the boundary of the contact area, and minimum at the center. (This distribution was also predicted by Engel.[4]) With blunt wedge-shaped solid bodies, the sharper the wedge angle, the greater is the pressure nonuniformity.

[3] P. Savic and G. T. Boult, Proc. Heat Transfer Fluid Mech. Inst., 1957, 43.
[4] Olive G. Engel, J. Res. Natl. Bur. Std. **54**, 281 (1955).
[5] Olive G. Engel, J. Res. Natl. Bur. Std. **64A**, 497 (1960).
[6] F. P. Bowden and J. E. Field, Proc. Roy. Soc. (London) **A282**, 331 (1964).
[7] R. Skalak and D. Feit, J. Eng. Ind. **88**, 325 (1966).

From these findings, it seems reasonable to infer the following for the impact of a liquid drop: The pressures are virtually uniform and equal to $\rho_0 C V_0$ at the first instant of contact, *but become more and more nonuniform, with their magnitude at the perimeter ever increasing, as the impact progresses and the contact angle ϕ increases.*

Once the limit of the initial stage has been reached, the shock front becomes detached and lateral outflow from the impact zone begins. The elastic energy in the compressed liquid is gradually transformed into kinetic energy of the lateral flow, and the contact pressures must decrease. The lateral outflow velocities can be very high: Lateral velocities which exceed the impact velocity V_0 by a factor of 2–5 have been experimentally observed by Engel,[4] Bowden and Brunton,[8] and Jenkins and Booker.[9]

While no rigorous analysis of the lateral "jetting" mechanism has been offered, Bowden and Brunton,[8] Laschimke,[10] and Field[11] have made the significant observation that the impact and flow phenomena in the vicinity of the interface perimeter are very similar to those which occur in the high-speed oblique collapse of two metal bodies or plates, as in explosive welding and cladding. In this process also, a high-speed jet is formed by what can be superficially regarded as a "wedging" or "extrusion" action between the collapsing bodies. The similarity extends even to the circumferential wrinkles often seen around the impact point of a liquid drop (see Ref. 8 or 10), and the wave-like nature of the welded joint in explosive cladding.[12]

The collapse process was first analyzed by Birkhoff *et al.*[13] in terms of an incompressible fluid flow model which predicts a jet formation under all conditions. Walsh *et al.*[1] have shown, however, that *no* jet is formed when the collapse angle ϕ is less than a critical angle ϕ_c. They formulated a compressible flow model in

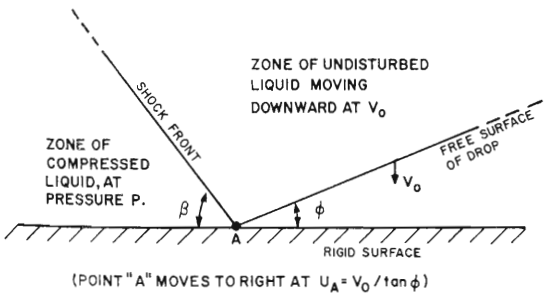

FIG. 2. Conditions at perimeter of contact area (point A in Fig. 1) during initial no-flow stage of impact.

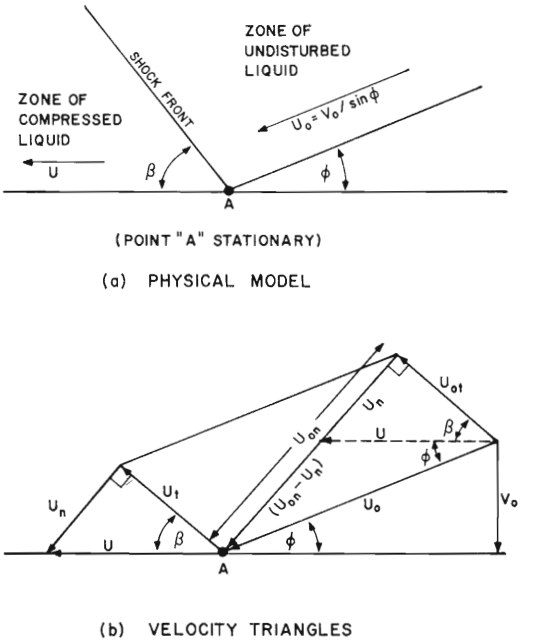

FIG. 3. Conditions at contact perimeter, point A, with translated coordinates.

which the deflection of the impacting plate is assumed to be caused by an oblique shock wave which is attached to the instantaneous collision point A (see Fig. 2). The critical angle is that condition at which this model is no longer tenable when the dynamics in the region *A* are analyzed. Evidently, the "jetless" model is closely analogous to the "initial stage" of droplet impact which has been described earlier, and the critical angle ϕ_c corresponds to the limit of this initial stage.

Recently, numerical time-incremented network approaches, such as the "Marker-and-Cell"(incompressible fluid) and "Particle-in-Cell" (compressible fluid) methods, have been applied to the impact and splash of fluid drops.[14] Neither of these, however, appears to be as yet applicable to the compressible response of a liquid drop at intermediate values of the Impact Mach Number V_0/C_0. Hopefully, extensions of these approaches will eventually be employed to obtain a complete rigorous solution of the phenomenon with which we are here concerned. Meanwhile, an approximate solution which at least approaches the three-dimensional condition should be of interest.

The remainder of this paper will be devoted to adapting the analysis of Ref. 1 to the droplet impact case, and to the discussion of the results so obtained.

III. THEORY

Basic Analytical Model

In the previous discussion we have argued that, in the impact of a liquid drop onto a rigid plane surface, there is an initial period in which the shock front cre-

[8] F. P. Bowden and J. H. Brunton, Proc. Roy. Soc. (London) **A263**, 433 (1961).
[9] D. C. Jenkins and J. D. Booker, in *Aerodynamic Capture of Particles* (Pergamon Press, Inc., New York, 1960), p. 97.
[10] R. Laschimke, Arch. Eisenhüttenw. **37**, 997 (1966).
[11] J. E. Field, in *Proc. Second Meersburg Conf. Rain Erosion and Allied Phenomena* (Royal Aircraft Establishment, Farnborough, England, 1968), Vol. 2, p. 751.
[12] A. S. Bahrani and B. Crossland, Proc. Inst. Mech. Engrs. **179**, 264 (1965).
[13] G. Birkhoff, D. P. MacDougall, E. M. Pugh, and G. I. Taylor, J. Appl. Phys. **19**, 563 (1948).
[14] F. P. Harlow and J. P. Shannon, J. Appl. Phys. **38**, 3855 (1967).

ated by the impact remains attached at the instantaneous contact perimeter, and no tangential outflow takes place. Furthermore, we have argued that during this stage the instantaneous contact pressures have a maximum at the contact perimeter. We would like to know how this pressure changes as the contact angle ϕ increases, and at what critical value of ϕ_c the shock front can no longer remain attached, and lateral flow begins. We assume intuitively that the pressure at the perimeter at that instant is the highest contact pressure experienced by the target as a result of the impact, and is therefore of primary interest.

The analysis which follows rests upon several simplifying assumptions. First, we assume that a reasonable approximation is afforded by a two-dimensional model, representing a thin parallel slice taken vertically through the impacting drop. (This would exactly represent the lateral impact of a liquid cylinder against a solid surface, as occurs many impingement erosion test devices.) Second, we assume that we may restrict our attention to a very small region surrounding the contact perimeter point A, as though the shock front passing through A were a semi-infinite plane. The model then reduces to that shown in Fig. 2, which is essentially the configuration treated by Walsh *et al.*,[1] whose approach we shall generally follow. Third, we assume that the fluid is inviscid and can slip along the solid surface, or that the consequences of a shear layer are negligible.

The next step is to translate to a coordinate system moving to the right at velocity $U_A = V_0/\tan\phi$, so as to hold the point A stationary, and thus to transform the model into a quasisteady flow configuration. Since in our problem ϕ and hence U_A vary with time, we must make the further assumption that this quasisteady point of view is justifiable. Reference 1 argues that this assumption is valid providing the angle ϕ increases with time, which of course is true in droplet impact.

The final model is shown in Fig. 3. Relative to the new coordinates, the undisturbed fluid has a velocity U_0, composed of components U_{0n} and U_{0t} normal and tangential to the shock front, respectively. The compressed fluid has a velocity U which must be parallel to the rigid target surface, and has components U_n and U_t normal and tangential to the shock front. As the fluid passes through the shock front, its tangential velocity component is assumed unchanged, so that

$$U_{0t} = U_t. \tag{5}$$

The velocities normal to the shock front, and the density and pressure changes across the shock front, are related by the usual Rankine–Hugoniot equations. Note that U_{0n} represents the velocity of propagation of the shock front relative to the undisturbed liquid, and $(U_{0n} - U_n)$ represents the particle velocity change across the shock front. Thus, the momentum relation is

$$P = \rho_0 U_{0n}(U_{0n} - U_n) \tag{6}$$

and the continuity relation is

$$\rho_0 U_{0n} = \rho U_n, \tag{7}$$

where P is the pressure rise across the shock front and ρ_0 and ρ are the densities of the undisturbed liquid and compressed liquid, respectively.

Equations (6) and (7) can be solved explicitly for U_{0n} and U_n, as follows:

$$U_{0n}^2 = P/\rho_0(1-\rho_0/\rho) \tag{8}$$

and

$$U_n^2 = P(\rho_0/\rho)^2/\rho_0(1-\rho_0/\rho). \tag{9}$$

We now nondimensionalize the above by introducing the notations $p = P/\rho_0 C_0^2$, $u_{0n} = U_{0n}/C_0$, $u_n = U_n/C_0$, and $q = 1-\rho_0/\rho$. The compression coefficient q is preferred over $\mu = (\rho/\rho_0) - 1$ as adopted by Ref. 1, because it results in tidier expressions and also because its maximum range lies between zero and unity rather than between zero and infinity. We thereby obtain

$$u_{0n}^2 = p/q \tag{10}$$

and

$$u_n^2 = p(1-q)^2/q. \tag{11}$$

If we can express p in terms of q by means of a suitable equation of state, then u_{0n} and u_n become functions of q directly. The equation chosen here is that consistent with the approximate shock-velocity–particle-velocity relationship proposed in Ref. 2, which states

$$C = C_0 + kV, \tag{12}$$

where V is the particle velocity change across a shock front, and k is a nondimensional constant. As shown in Appendix I, Eq. (12) implies that

$$p = q/(1-kq)^2. \tag{13}$$

Substituting Eq. (13) in (10) and (11) gives the more direct expressions:

$$u_{0n} = 1/(1-kq) \tag{14}$$

and

$$u_n = (1-q)/(1-kq). \tag{15}$$

The remaining velocities and the angle ϕ can be found by geometry from Fig. 3, and formulated in terms of the "Impact Mach Number" $M_0 = V_0/C_0$ and the nondimensional velocities $u_0 = U_0/C_0$ and $u_t = U_{0t}/C_0 = U_t/C_0$. This results in

$$u_t^2 = u_0^2 - u_{0n}^2, \tag{16}$$

$$u^2 = u_t^2 + u_n^2, \tag{17}$$

$$\phi = \tan^{-1}(u_{0n}/u_t) - \tan^{-1}(u_n/u_t), \tag{18}$$

or

$$\phi = \tan^{-1}[u_t(u_{0n} - u_n)/(u_t^2 + u_{0n}u_n)], \tag{19}$$

$$M_0 = u_0 \sin\phi. \tag{20}$$

Note that these equations do not permit us to choose M_0 and ϕ as the independent parameters directly; rather, q and u_0 must be assumed, and ϕ and M_0 follow from Eqs. (18) or (19) and (20).

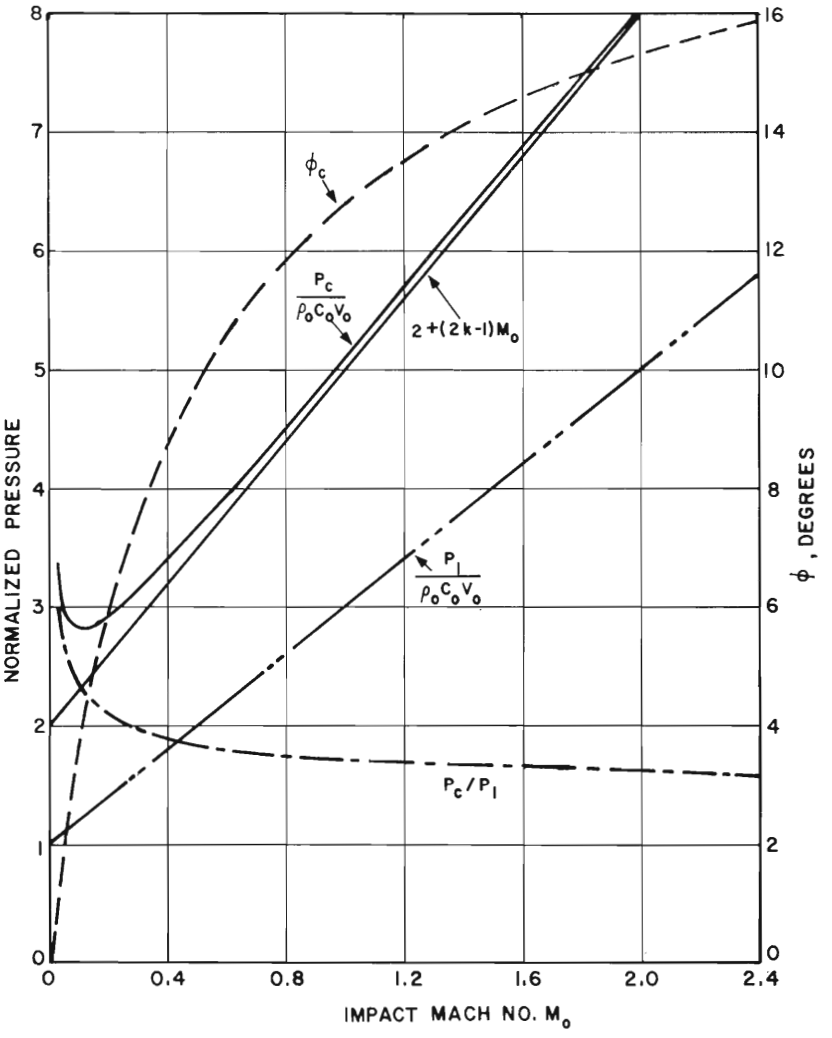

FIG. 4. Critical conditions for $k=2$ (water).

Calculations for Critical Angle

If u_0 is held constant and q is gradually increased, the resulting values of ϕ first increase, pass through a maximum, and then decrease. (The corresponding changes in the various velocity components can be graphically presented by means of a "shock polar diagram," such as Fig. 3 of Ref. 1.) This points out two significant facts: Firstly, the maximum value of ϕ so obtained must be the critical value ϕ_c corresponding to the assumed u_0. Any value of ϕ greater than ϕ_c is not consistent with the assumed analytic model and therefore corresponds to a condition in which lateral jetting flow must be occurring. Secondly, for any value of ϕ less than ϕ_c, there are two values of q which satisfy the assumed conditions. These represent a "weak shock" and a "strong shock," respectively. Intuitively, we are interested in the lower value of q, or the "weak shock" solution, since, as ϕ physically increases, we expect the pressure and hence q to increase.

The value of q_c, corresponding to the critical angle ϕ_c, can be determined analytically be setting $\partial(\tan^2\phi)/\partial q=0$ and solving for q. Using Eqs. (19), (14), (15), and (16) we obtain

$$\tan\phi=q[u_0^2(1-kq)^2-1]^{1/2}/[u_0^2(1-kq)^2-q]. \quad (21)$$

This leads to a quadratic with the soluion

$$q_c=\frac{k(2u_0^2+1)\pm[u_0^2(8k^2-4k)+(k^2+4k)]^{1/2}}{2k(ku_0^2+1)}. \quad (22)$$

A numerical example shows that the minus sign in the above equation leads to the physically meaningful solution. The values of ϕ_c, p, M_0, and so on, corresponding to the critical condition, can then be readily calculated from the equations given earlier.

It must be acknowledged that the foregoing procedure obtains each critical point by assuming u_0 to be held constant while q is increased until ϕ reaches a maximum, so that M_0 changes as q and ϕ change. But our real interest is in the maximum value which ϕ attains as q increases with M_0 held constant, during which process u_0 must decrease. However, if we are justified in assuming that the "quasisteady-state" analysis is valid, then it does not matter by which "path" a critical condition is approached. The result should still be physically

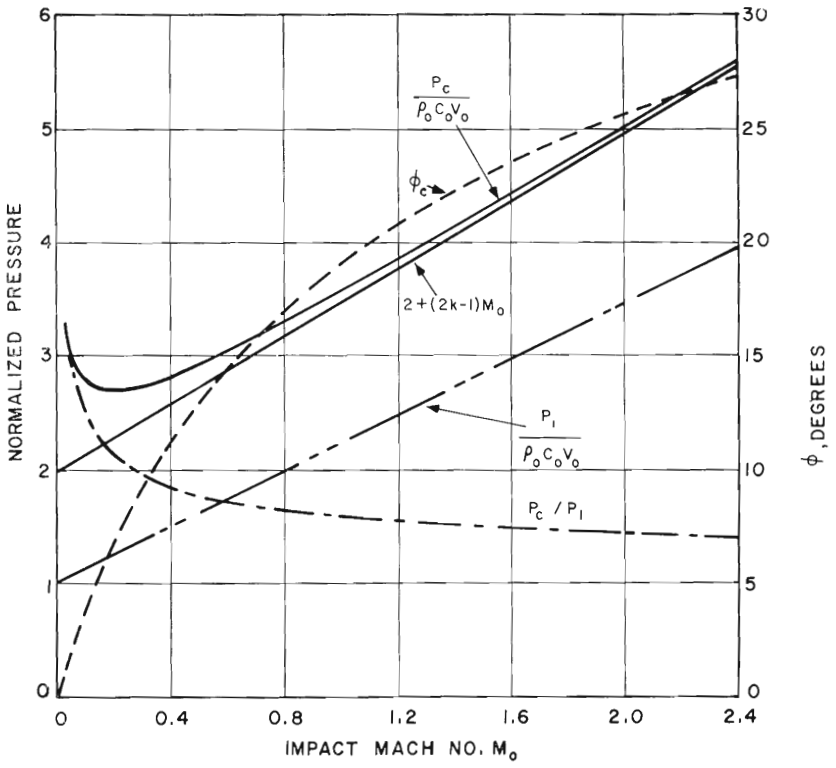

FIG. 5. Critical conditions for $k=1.242$ (sodium).

correct. Thus, critical values can be calculated by the manner described, and plotted against the calculated values of M_0 rather than against the assumed values of u_0.

Calculations for Noncritical Angles

The pressures and angles at the critical conditions are perhaps the most important results to be sought. But we should also like to have plots of p versus ϕ at given values of M_0, to show how the pressure at the contact edge varies as the liquid/solid interface grows. The procedure, following Ref. 1, is to obtain one point by assuming values of k, u_0, and q, and calculating in turn p, u_{0n}, u_n, u_t, ϕ, and M_0 from Eqs. (13)–(16), (18), and (20), respectively. After repeating this for different values of q, one can interpolate graphically or analytically to determine the values of ϕ, p, and so on for arbitrarily chosen values of M_0. Going through the same procedure with different assumed values of u_0 leads to a second point for each chosen value of M_0 and so on. Thus, the desired information can be compiled for a given fluid, represented by its given value of k. (More elegant iterative procedures can be envisioned, but we were not successful in developing a successful one in the time available to us.)

IV. DISCUSSION OF RESULTS

The calculation methods described in the previous section were programmed in FORTRAN IV, for a CDC-6400 computer, and results will be given for $k=2.0$ and 1.242. The value $k=2$ fits the data for water up to about $M_0=1.2$, as shown in Ref. 2. Values $k=1.242$ and $k=1.188$ have been given by Rice[15] for sodium and potassium, respectively. In order to facilitate comparison with earlier theories, pressures are normalized with respect to the one-dimensional low-speed waterhammer approximation, given by Eq. (1). Thus, the numerical values represent the ratio $P/\rho_0 C_0 V_0$ or p/M_0.

Results for critical conditions are plotted against "Impact Mach Number" $M_0=V_0/C_0$ on Figs. 4 and 5. Besides the plot of the critical angle ϕ_c itself, four pressure plots are shown. One is the normalized pressure corresponding to the critical angle $P_c/\rho_0 C_0 V_0$. Another is the normalized pressure calculated by the one-dimensional theory of Ref. 2, which, from Eq. (2) can be written as $P_1/\rho_0 C_0 V_0=1+kM_0$. The ratio P_c/P_1 is also plotted, since it represents the correction factor attributable to the drop roundness effect. The fourth pressure line is that given by the equation

$$P_2/\rho_0 C_0 V_0=2+(2k-1)M_0. \tag{23}$$

Equation (23) was established inductively by inspection of Figs. 4 and 5, and provides a reasonable approximation to the critical pressure in each case, provided $M_0>0.2$. The writer has not yet succeeded in deriving this simple approximation analytically.

Two other interesting generalized observations can be made: First, $P_c/\rho_0 C_0 V_0$ exhibits a minimum in the region of $M_0=0.1$–0.2, and sharply increases as M_0 diminishes towards zero. This, of course, does not mean

[15] M. H. Rice, J. Phys. Chem. Solids **26**, 483 (1965).

that the pressure P_c itself increases with decreasing M_0; in fact, P_c also decreases towards zero. What it does mean is that the correction due to the drop roundness effect (P_c/P_1) is greatest at small values of M_0. On the other hand, the correction due to the pressure dependence of C, given by $P_1/\rho_0 C_0 V_0$, increases with M_0. These opposing trends lead to a minimum in the combined correction.

The second observation is that the critical angle ϕ_c is smaller than predicted by the simplified model of Bowden and Field,[6] Eq. (4). This equation, with the substitution of $C=C_0(1+kM_0)$ from Eq. (12) becomes

$$\sin\phi_1 = V_0/C = M_0/(1+kM_0). \qquad (24)$$

The values of ϕ_1 and ϕ_c, for $k=2$, have been plotted on Fig. 6 to show their difference. The reason for this difference is that Bowden and Field assumed the shock front to be normal to the drop surface at the critical condition; that is, its velocity U_0 along the drop surface was assumed to be the shock propagation velocity C. But Fig. 3(b) shows that this is physically impossible: If the angle $(\beta+\phi)$ were 90°, U_n and U would have to be zero; in other words, there would be no flow *out* of the stationary shock wave although there is flow *into* it. The angles β_c and $(\beta+\phi)_c$ are also plotted on Fig. 6. The latter is seen to reach a constant value of about 55° above $M_0=1.2$. It can be shown analytically that, for large values of u_0, $\cot(\beta+\phi)_c=[(k-1)/k]^{1/2}$.

Experimental confirmation of the angle ϕ_c here predicted is lacking. Measurements of the spreading flow from the impact of a falling waterdrop were reported by Engel,[4] but the impact velocity was very low (28 ft/sec) and the exact stage at which flow initiated was not determined. Hancox and Brunton[16] sought to deduce the angle ϕ_c from measurements of the distance between the center of the impact and the location at which shear damage, attributable to high-speed tangential flow, is first observed. Surprisingly, the angles deduced in this manner proved to be essentially independent of impact velocity and even of the liquid used (mercury or water), and much greater than predicted, even by Eq. (24). The measured values were around 17°. While no complete explanation of Hancox and Brunton's findings are offered here, there are good reasons for not expecting them to agree with our theoretical predictions. First, the solid target material was polymethylmethacrylate ("lucite"), whose acoustic impedance is on the same order-of-magnitude as that of water. Thus the dynamic elastic deformations will be on the same order-of-magnitude in the solid as in the liquid, and a theory which assumes the target to be rigid is certainly not applicable. Second, the critical condition is that at which the shock front just detaches from the solid surface, and jetting flow just begins. The thickness of the jet surely must grow to some finite value before its damaging potential becomes significant,

[16] N. L. Hancox and J. H. Brunton, Phil. Trans. Roy. Soc. London, Ser. A **260**, 121 (1966).

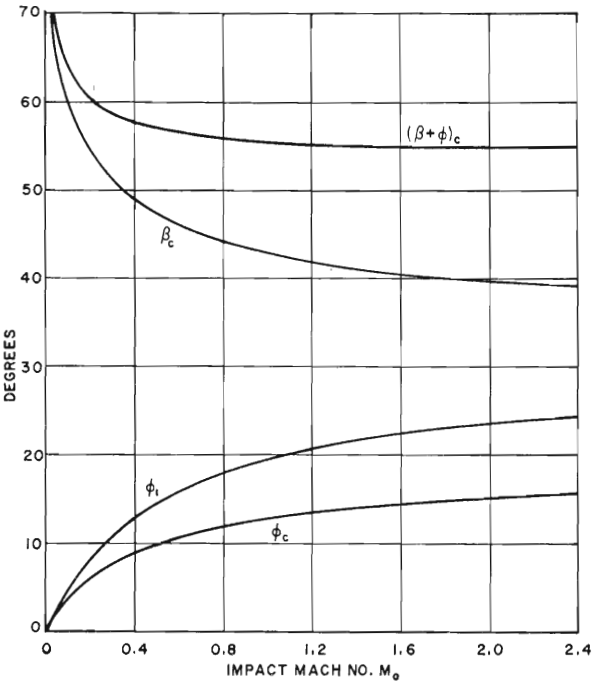

FIG. 6. Critical angles, $k=2$.

by which time the angle ϕ (if it can still be defined) will have grown beyond the critical value.

Let us now discuss the magnitudes of the critical pressures, which, as stated earlier, should represent (or at least approximate) the maximum instantaneous pressures generated during the primary impact process. For water (Fig. 4) the *minimum* value of $P_c/\rho_0 C_0 V_0$ is about 2.8, and, in fact, the value

$$P_c = 3\rho_0 C_0 V_0 \qquad (25)$$

can be used as a good approximation for all impacts in the medium speed range, say from $M_0=0.03$ (150 ft/sec), to $M_0=0.35$ (1750 ft/sec). This range encompasses most experiments carried out in steam turbine blade erosion research.

Again, direct experimental comparison is not available, due to the difficulty of measuring surface stresses so localized and so fleeting as those under consideration. There have been a number of attempts to deduce pressures indirectly, but in many instances these represented average rather than maximum pressures, calculated from total load measurements.

One approach toward deducing maximum pressures is afforded by the hypothesis that erosion due to repeated liquid impacts is a fatigue-like process. If this hypothesis is correct (and it is supported by numerous metallurgical studies of erosion fractures) then an analogy can be postulated between the "threshold impact velocity" V_t below which no erosion occurs, and the stress endurance limit σ_e below which no fatigue failures occur. An exact correspondence should not be expected, since the stress distribution, the stress cycling

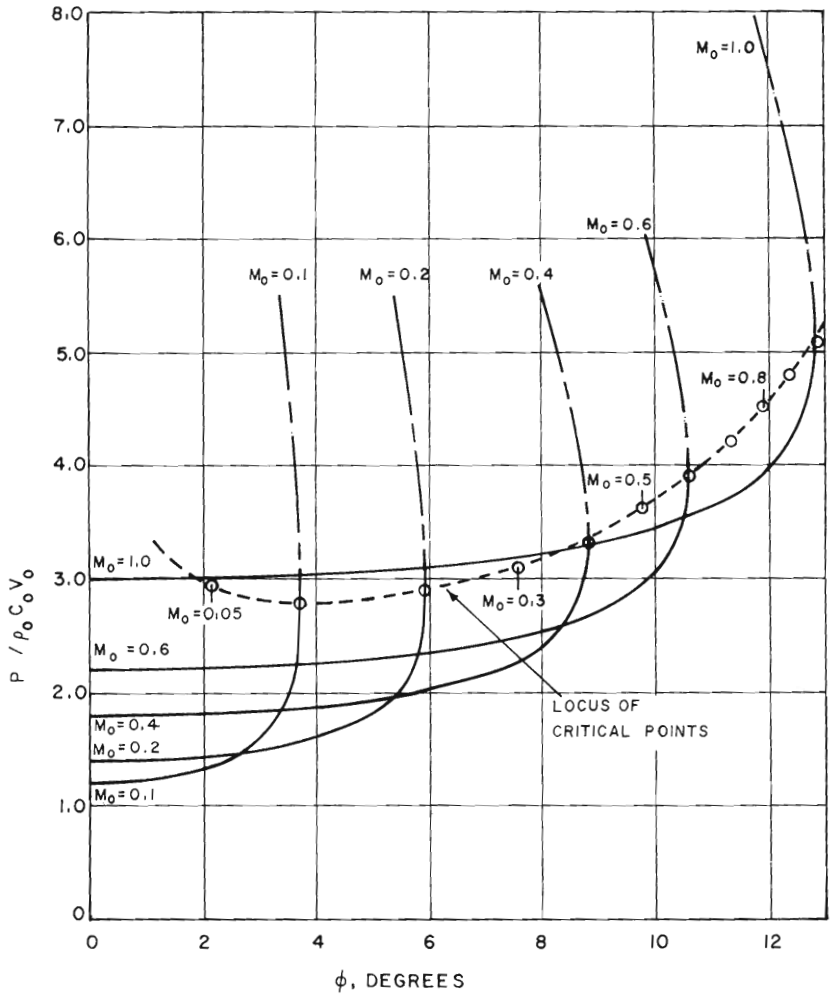

FIG. 7. Edge pressure vs contact angle, $k=2.0$.

history, and the strain rate in each stress application, are all quite different under repeated droplet impact than under conventional fatigue test conditions. Nevertheless, a rough agreement with Eq. (25) would be encouraging. A comparison of erosion threshold velocities and endurance limits, from several sources, has been presented by Thiruvengadam.[17] His findings were reasonably consistent with Eq. (25): values of $\sigma_e/\rho_0 C_0 V_t$ ranged from 1.8 to 2.1. An additional datum is provided by Thomas,[18] whose result for mild steel can be expressed as $\sigma_e/\rho_0 C_0 V_t = 2.7$.

Maximum impact pressures on the order of $2\ \rho_0 C_0 V_0$ or higher have also been deduced by Jolliffe,[19] from measurements of "dislocation rosettes" produced by single droplet impacts on freshly cleaved lithium fluoride crystals.

The preponderance of experimental evidence, circumstantial though it may be, therefore supports the conclusion that the maximum impact pressure due to a liquid drop on a rigid surface is approximated by Eq. (25). This pressure is 15 times as high as the value obtained from Eq. (4), with $\alpha=0.41$ for a rigid target, which has been widely quoted in the literature as representing the maximum pressure.

Finally, let us examine the manner in which the pressures at the contact perimeter vary, from the initial moment of contact until the critical condition is reached and jetting initiates. Curves of $P/\rho_0 C_0 V_0$ versus ϕ, with M_0 as a parameter, are presented for $k=2$ on Fig. 7 and for $k=1.242$ on Fig. 8. For each value of M_0, the pressure at $\phi=0$ is equal to the one-dimensional pressure according to Eq. (2). This is just what we should expect since, at very low values of ϕ, the radius of curvature of the drop is so large compared to the radius of the contact area that, for practical purposes, conditions can be considered one dimensional. The pressure curves become increasingly steep as ϕ increases, eventually reaching a vertical slope and doubling backwards, with ϕ now diminishing as the pressure

[17] A. Thiruvengadam, in *Erosion by Cavitation or Impingement, STP 408* (American Society for Testing and Materials, Philadelphia, 1967), p. 22.

[18] G. P. Thomas, in *Proc. Second Meersburg Conf. Rain Erosion and Allied Phenomena* (Royal Aircraft Establishment, Farnborough, England, 1968), Vol. 2, p. 785.

[19] K. H. Jolliffe, Phil. Trans. Roy. Soc. London, Ser. A **260**, 101 (1966).

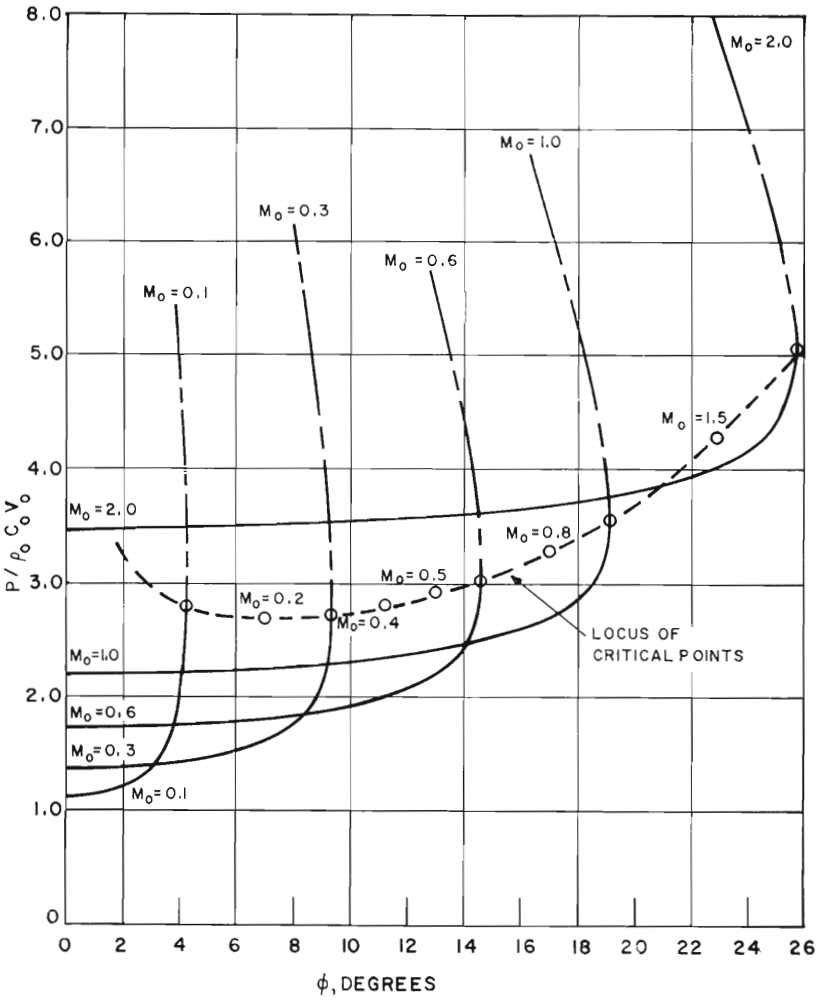

FIG. 8. Edge pressure vs contact angle, $k = 1.242$.

further increases. This is consistent with our earlier discussions: The maximum value of ϕ reached is, of course, the critical angle ϕ_c, and the corresponding pressure is the critical pressure P_c. The portion of the curve for higher pressures corresponds to the "strong shock" solution, which we have rejected on physical grounds. The loci of critical points, i.e., the values of $P_c/\rho_0 C_0 V_0$ versus ϕ_c, from the earlier results of Figs. 4 and 5, are shown as dotted lines on Figs. 7 and 8.

Note that the one-dimensional pressure, according to Eq. (2), remains a good approximation of the edge pressure until the contact angle ϕ has reached about half of its critical value. During that phase of the impact process, the pressure distribution over the contact area may be taken to remain substantially uniform.

V. SUMMARY AND CONCLUSIONS

Heretofore there had existed no reliable information on the maximum pressure developed in the impact between a round liquid drop and a plane solid surface. Most estimates have been based on one-dimensional analyses which are not strictly applicable. In this paper a closer approximation to the physical three-dimensional case is presented, in which the conditions existing at the instantaneous perimeter or edge of the contact area are treated in a quasisteady two-dimensional manner. This approach has been adapted from a somewhat related analysis of Walsh *et al.*[1] and makes use of an equation of state consistent with the one-dimensional analysis of Heymann.[2]

The analysis is valid only for the initial phase of impact, during which the expanding shock front generated by the impact still remains attached to the target surface, so that no lateral "jetting" or spreading can occur. A major result of the analysis is the evaluation of the critical contact angle ϕ_c between drop surface and target, at which the above assumption breaks down and lateral jetting must be assumed to begin. The critical edge pressure P_c, corresponding to that angle, is assumed to constitute the maximum pressure generated by the impact. Another result of the analysis is the variation of the edge pressure as ϕ increases from the initial instant of point contact until the critical condition is reached.

Quantitative results have been presented for two values of the liquid shock velocity coefficient k, namely $k=2.0$ (water) and $k=1.242$ (sodium). These results may be summarized as follows:

The edge pressure remains substantially equal to the one-dimensional pressure until the contact angle ϕ has reached about half its critical value ϕ_c. Then the pressures rises at an increasing rate, and $\partial P/\partial\phi$ becomes infinite when the critical condition is reached. The critical pressure for water can be roughly approximated by $P_c=3\rho_0C_0V_0$ in the impact velocity range $0.03\leq V_0/C_0\leq 0.3$. For sodium and potassium, the corresponding approximation $P_c=2.8\rho_0C_0V_0$ applies in the range $0.05\leq V_0/C_0\leq 0.5$. At high impact velocities, the critical pressure is approximated by the expression $P_c/\rho_0C_0V_0=2+(2k-1)(V_0/C_0)$. These pressures are far higher than have heretofore been supposed in most of the relevant literature, although circumstantial experimental evidence supports the present results. It is noteworthy that the drop roundness effect, represented by the ratio of P_c to the one-dimensional impact pressure at the same conditions, is greatest at low velocities, tending toward infinity as V_0/C_0 tends toward zero. At high velocities, this ratio is on the order of 1.5.

The analysis here presented gives no information about the pressure distribution within the instantaneous contact area, but previous related work suggests that this is nonuniform, the pressure in the center of the contact area being the lowest. There is still a need, however, for a complete and rigorous analysis of the three-dimensional liquid–solid impact problem. This would probably require a time-incremented numerical approach, such as the "Particle-in-Cell" method, adapted for a suitable equation of state and a suitable Mach number domain.

ACKNOWLEDGMENTS

The author would like to express his indebtedness to Dr. J. H. Brunton and Dr. J. E. Field, of the University of Cambridge, for pointing out to him the similarities between the droplet impact and explosive welding phenomena, and acquainting him with some of the literature on the latter. Without that stimulus, this work would probably not have been done. The author also would like to thank Mr. W. F. Stahl for constructive criticism and Mr. E. L. Phelts for writing the computer programs which generated the numerical results.

APPENDIX: EQUATION OF STATE

Reference 2 presented a simple physical argument for an approximate relationship between shock velocity C and particle velocity V, of the form

$$C/C_0=1+k(V/C_0) \tag{A1}$$

and showed that this provided a quite accurate fit to the exact data for water up to about $V/C_0=1.2$, with $k=2$. Other confirmation for such a linear formulation has been given by Rice,[15] Ruoff,[20] and Jones *et al.*[21] It seems reasonable, therefore, to adopt the equation of state implied by Eq. (A1).

The continuity equation across a shock can be expressed as

$$V/C=1-(\rho_0/\rho)=q. \tag{A2}$$

From Eqs. (A1) and (A2) we obtain

$$C/C_0=1/(1-kq) \tag{A3}$$

and

$$V/C_0=(V/C)(C/C_0)=q/(1-kq). \tag{A4}$$

The momentum equation across a shock front can be put into the form

$$P/\rho_0C_0^2=(C/C_0)(V/C_0) \tag{A5}$$

which, with (A3) and (A4) substituted, becomes

$$p=P/\rho_0C_0^2=q/(1-kq)^2. \tag{A6}$$

This is our desired equation of state. We may ask what its limit of validity is for water, since Eq. (A1) becomes increasingly inaccurate above $V/C_0=1.2$. Figure 1 of Ref. 2 shows that at $V/C_0=2$, the true value of C/C_0 is about 4.5, versus 5.0 from Eq. (A1). The corresponding true value of $P/\rho_0C_0^2$ is 9, versus a calculated value of 10. Thus, the error in Eq. (A6) is only on the order of 10% even at values of $P/\rho_0C_0^2$ as high as 10. This error is probably smaller than other errors introduced by the simplifying assumptions in the physical model here adopted.

[20] A. L. Ruoff, J. Appl. Phys. **38**, 4976 (1967).
[21] A. H. Jones, W. M. Isbell, and C. J. Maiden, J. Appl. Phys. **37**, 3493 (1966).